Microstructure and mechanical properties of $(AlTi)_xN_{1-x}$ films by magnetic-field-enhanced high power impulse magnetron sputtering

Xiubo Tian,[a] Yinghe Ma, Jian Hu, Mingkang Bi, and Chunzhi Gong
State Key Lab of Advanced Welding and Joining, Harbin Institute of Technology, Harbin 150001, China

Paul K. Chu
Department of Physics and Materials Science, City University of Hong Kong, Tat Chee Avenue, Kowloon, Hong Kong, China

(Received 11 August 2016; accepted 14 November 2016; published 19 December 2016)

Compared to conventional direct current magnetron sputtering, high power impulse magnetron sputtering (HiPIMS) gives rise to higher plasma activity which can be exploited to deposit films with the preferred microstructure and higher critical load, but in practice, most of the electrons are not effectively utilized and lost to the anode (chamber wall). In order to achieve higher ion flux to substrate and denser microstructure of the films, an external magnetic field is introduced. In our HiPIMS system, a coil around the magnetron target induces larger enhancement effects, and the substrate current can be increased by a factor of 2 or more if the proper current flows through the coil to intensify and confine the glow discharge. The magnetic-field-enhanced HiPIMS technology is adopted to produce $(AlTi)_xN_{1-x}$ films with smooth surfaces and better mechanical properties such as surface hardness and a larger coil current produces films with lower friction. The improvement is attributed to enhanced glow discharge, more nitrogen incorporation, and intense ion bombardment. © *2016 American Vacuum Society*. [http://dx.doi.org/10.1116/1.4971202]

I. INTRODUCTION

Magnetron sputtering (MS) is widely used in coating fields. However, compared to arc-based techniques, MS is featured by the lower ionization of sputtered atoms and lower plasma density near the samples, which result in insufficient adhesion between the coating and substrate.[1] In high power impulse magnetron sputtering (HiPIMS),[2–5] a larger pulse current is generated between the magnetron target and anode to achieve a plasma density that can be 2–3 orders of magnitude higher than that in conventional DC magnetron sputtering. This is accomplished by applying electrical pulses of up to megawatt power to the target, but a small duty cycle is often used due to limitation in the power supply and heat input into the magnetron target.[6,7] Unfortunately, HiPIMS suffers from some drawbacks in spite of the higher plasma density, better film adhesion, and more uniform film thickness.[8] Unwanted arcing occurs more frequently and the deposition rate is smaller than that in direct current magnetron sputtering for the same average power.[9] Narrower HiPIMS pulses may lead to larger deposition rates[10] which can also be increased by reducing the magnetic field strength.[11] Nonetheless, HiPIMS still produces a smaller density (10^{18}–$10^{19}/m^3$) than a vacuum arc (10^{18}–$10^{21}/m^3$) in general.[12]

In this study, electrical coils are installed on the HiPIMS target outside the vacuum chamber to produce an external magnetic field to enhance glow discharge and deposition rate.[13] The effects of the external magnetic field on the glow discharge characteristics as well as the microstructure, deposition rate, mechanical properties, and adhesion of $(AlTi)_xN_{1-x}$ films[14,15] are investigated in details.

II. EXPERIMENTAL DETAILS

HiPIMS deposition was performed in a magnetron sputtering chamber with dimensions of Ø400 × 400 mm, as shown in Fig. 1. Four cathodes with dimensions of Ø50 × 7 mm (only two cathodes used in the experiment) were installed on the chamber wall. The magnetron discharge was triggered by a custom hybrid HiPIMS power supply[16] operating in three modes: DC, pulse, and DC + pulse. The DC + pulse mode offering stable operation with less arcing and higher ionization and deposition rates was implemented in our experiments. The power supply was operated at a maximum voltage of 1000 V and current of 400 A. The coils were installed outside the chamber wall to generate the magnetic field to increase the plasma density in the vicinity of the samples. Two cathodes (Ti50Al50 and Cr) were used. Mirror-polished M2 steel acted as samples with dimensions of Ø20 × 3 mm and silicon was also utilized as substrate for SEM, x-ray diffraction (XRD), and AFM analysis. The processes were performed according to the following steps: (1) argon ion cleaning, (2) Cr layer deposition, (3) CrN layer deposition, and (4) $(AlTi)_xN_{1-x}$ layer deposition, as illustrated in Table I. The pulse duration and frequency were 100 μs, 150 Hz and 200 μs, 50 Hz, respectively, for plasma-cleaning and film deposition. The Ti50Al50 target was excited with the average power of 200 W (in case of no coil current) and pulse peak power density of approximately 1 kW/cm^2 in the experiment. The sample temperature greatly affects the microstructure and surface properties.[17] In this experiment, the sample temperature was kept at

[a]Author to whom correspondence should be addressed; electronic mail: xiubotian@163.com

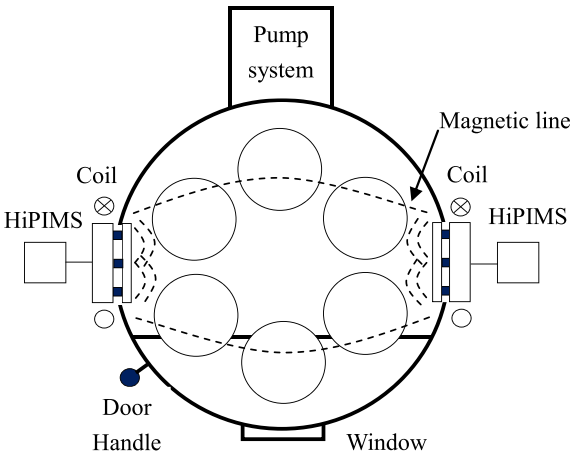

FIG. 1. (Color online) Schematic of the hybrid HiPIMS system.

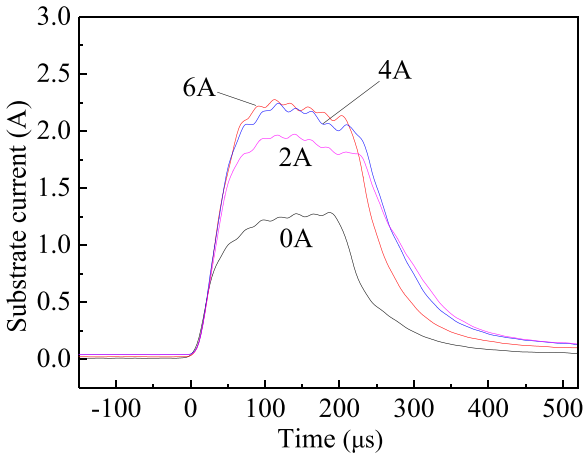

FIG. 2. (Color online) Dependence of the substrate current on coil current producing the magnetic field.

approximately 450 °C for only studying the effect of magnetic field. In fact, the influence of sample temperature on film microstructure under the external magnetic field should be investigated later.

The surface microstructure and thickness of the deposited films were examined by a Quanta 200FEG high-resolution field-emission scanning electron microscope (FEI), and the chemical composition was determined on a high-resolution electron microprobe. The surface topography was assessed by atomic force microscopy (Dimension Icon) from a scanned area of $5 \times 5\,\mu$m. Structural analyses were conducted by XRD with Cu K_α radiation on a Panalytical diffractometer. The hardness and Young's modulus were measured using MTS Nano Indenter XP at a maximum indentation depth of 100 nm. The friction coefficients were determined on a ball-on-disk wear apparatus at a rotation speed of 80 rpm and loading of 100 g with a 6 mm diameter ZrO_2 ball.

III. RESULTS AND DISCUSSION

The currents flowing through the substrate during $(AlTi)_xN_{1-x}$ deposition for different coil currents (i.e., different magnetic fields) are shown in Fig. 2. The pulse current rises rapidly in the first 30–50 μs and decreases gradually in the next 80–100 μs due to energy consumption in the power-supply capacitor tank. The long current tail indicates that the large plasma density will last for a long time, even 300 μs after HiPIMS pulse-off. The coil current affects the substrate current. A larger substrate current is induced by the external magnetic field, implying that the magnetic field increases the plasma density near the substrate. Anders *et al*. have added a solenoid between the MS target and substrate to produce a positive effect[18] and the solenoid generates an axial magnetic field affecting the degree of unbalancing the magnetron and the plasma can escape from the target region at an enhanced rate. The magnetic field also enhances excitation and ionization and guides the plasma toward the substrate. In this way, a high-density plasma appears in front of the sample. In fact, the magnetic field is capable of magnetizing electrons, but ions are difficult to magnetize due to the larger mass. Consequently, electrons are moved by the magnetic field. However, even a small charge separation in the plasma may generate an internal field and the associated electrostatic force will keep the electrons and ions together (bipolar diffusion). The combined effect of electron movement by the magnetic field and ion guiding by the electric field in the plasma dictates the flow of the plasma.[19] As a result, most of generated plasma moves toward the substrate under the external magnetic field thus producing the larger bias current as shown in Fig. 2. Once the discharge is pulse off, the confined ions are depleted quickly, and the substrate current drops rapidly, especially for a larger coil current whose magnetic field confines more plasmas.

When the coil current is less than 4 A, the glow discharge is enhanced by the external magnetic field and the effects are slightly apparent if the coil current is increased to 6 A as

TABLE I. Instrumental parameters in HiPIMS process.

Processes	HiPIMS pulse current (A)	Additional DC current (A)	Ar flow (sccm)	N_2 flow (sccm)	Pressure (Pa)	Bias (V) and duty cycle (%)	Time (min)	Coil current (A)
Precleaning	0	0	30	0	2.5	−600 (50%)	30	5
Cr layer	10	0.25	30	0	0.5	−600 (50%)	20	4
CrN layer	15	0.25	24	6	0.5	−75 (60%)	30	4
$(AlTi)_xN_{1-x}$ layer	20	0.25	24	6	0.5	−75 (60%)	60	0
								2
								4
								6

shown in Fig. 2. The "saturation" effect of the magnetic field appears as reported by Jager *et al.*[19] that the floating potential in the solenoid does not change significantly when the DC flowing through the coil is increased from 138 to 337 A. It may be because most of the plasma is confined at a larger magnetic field. The magnetic field also affects the current waveforms. In the absence of an external magnetic field (coil current of 0 A), the substrate current rises gradually until the end of the HiPIMS pulse. In contrast, the current reaches the peak more rapidly if a current flows through the coils. The magnetic field may force more electrons to move to the front of the target and a more negative potential is induced. This high potential (negative) makes the electrons escape rapidly due to larger repulsion effect of the electric field. In this way, the high-density plasma reaches the sample quickly on account of the bipolar diffusion effect and the substrate rapidly receives the peak current. Afterward a current decrease is observed. It may be attributed to gas rarefaction effect which leads to a lower discharge current.[20]

Figure 3 shows the elemental concentration as a function of the coil current. The measure error is less than 2.5% and not shown here. The Al concentration is larger than that of titanium. This was also reported by Chen *et al.* using Ti50Al50 target.[21]

Generally, sputter erosion from the compound target will produce an identical ratio of emitted Ti to Al atoms with that of the bulk target composition. The compositional deviation between the films and the target mainly derives from the different angular and scattering losses of Al and Ti.[21] The variation may also be related to the different affinities of Ti and Al to nitrogen. The Gibbs free energy of TiN of $\Delta G^0_{TiN} = -308.3$ kJ/mol is more negative than that of AlN of $\Delta G^0_{AlN} = -287.0$ kJ/mol.[22] Consequently, Ti in the Al50Ti50 target is more easily poisoned than Al, and sputtering occurs more easily from weakly poisoned aluminum microzones.[21] The nitrogen concentration is lower in the film deposited without the external magnetic field because of the smaller ratio of nitrogen to argon as well as fewer nitrogen ions. When an external field is applied, the nitrogen content in the film increases with the coil current. The magnetic field enhances not only ionization of the sputtered particles, but also excitation and ionization of nitrogen. A higher nitrogen plasma density promotes the reaction between nitrogen and metallic elements to form near-stoichiometric nitride. The electrons in the plasma reach the anode (chamber wall) rapidly if not confined by the external field, but in the presence of a magnetic field, they are forced to travel a longer distance before hitting the wall. Consequently, ionization is enhanced and a larger coil current intensifies ion bombardment effects to produce denser and more compact films. If the coil current is further increased, the nitrogen concentration decreases as a result of the weaker discharge due to the higher plasma resistance induced by large field.

The $(AlTi)_xN_{1-x}$ film fabricated with the magnetic field has a finer structure which becomes denser and featureless at a larger coil current (e.g., 4 A) but becomes coarse when the coil current reaches 6 A although it is still more compact than that prepared without applying a coil current as shown in Fig. 4.

This may arise from more ion bombardment and different elemental composition. Tonshoff *et al.* have shown in high ion sputtering (HIS), the ion flux is more than twice that in magnetron sputter ion plating technology thereby producing a homogeneous and compact structure with a smooth surface and large microhardness.[23] By using HIS which provides a higher degree of ionization, "dimpled" coatings can be prepared on rough substrates even after a blasting treatment.[24] Bouzakis *et al.* have observed film densification and improvement of the life time of milling tools.[25] In our experiments, the plasma density near the substrate is further improved due to the confinement of magnetic field. This may be helpful for the films with better microstructure and properties.[26]

The deposition rate is affected by the magnetic field. The thicknesses of the films deposited using coil currents of 0, 2, 4, and 6 A are 1.42, 1.52, 1.54, and 1.63 μm for the same time as shown in Table I.

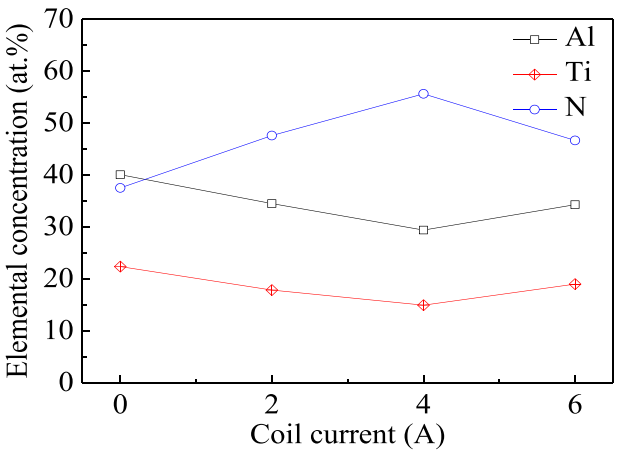

FIG. 3. (Color online) Elemental concentration as a function of coil currents.

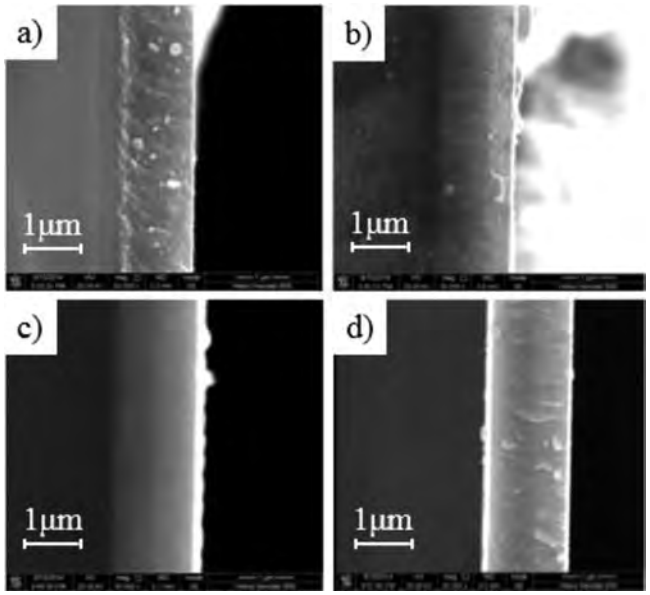

FIG. 4. Effect of coil currents on the thickness and structure of the $(AlTi)_xN_{1-x}$ films: (a) 0 A, (b) 2 A, (c) 4 A, and (d) 6 A.

Hence, the external magnetic field can be utilized to increase the deposition rate in HiPIMS because less materials are lost to the chamber wall.[27] It is noted that a higher magnetic field does not necessarily increase the deposition rate directly and the deposition rate has been reported to be independent of the magnetron configuration in a dual magnetron syste.[28] However, the magnetic field affects the ion current and consequently the ion-to-atom ratio. Bohlmark *et al.* have observed that the deposition rate can vary on different parts of the sample.[27]

Figure 5 depicts the XRD spectra of the $(AlTi)_xN_{1-x}$ samples revealing peaks stemming from CrN (300), TiAlN (200), TiN (220), AlN (100), etc. The crystallinity becomes better if a magnetic field is used. Owing to the larger plasma density, the mobility of adatoms on the substrate is better and atomic rearrangement is easier. When a coil current of 6 A is used, the AlN phase appears. The coil current affects the degree of unbalancing magnetic field,[29] discharge area on the target, ratio of ion to metal flux and subsequently the film microstructure.[21] More ion bombardment induced by larger magnetic field promotes the movement of atoms, which may contribute to the formation of stable AlN phase. The crystal size is calculated by the Scherrer equation[30] and in the presence of the magnetic field, the crystallite size deceases by 50%.

The surface roughness values of the films are 8.7, 7.1, 5.2, and 6.7 nm for coil currents of 0, 2, 4, and 6 A, respectively, as shown in Fig. 6.

The sample prepared without the external magnetic has a rougher surface and coarser structure whereas the film deposited at coil current of 4 A exhibits the lowest roughness. It may be attributed to different incorporation of nitrogen and ion bombardment effects. HiPIMS without the external magnetic field produces weak ion bombardment as indicated by lower substrate current (as shown in Fig. 2). However, in pulsed DC magnetron sputtering or low-power HiPIMS, a dense structure is still observed although the columnar morphology is only faintly observed.[31] When the coil current is increased (e.g., to 2 A), more nitrogen is incorporated into the film and a larger power input to sample (indicated by larger substrate current) changes the surface

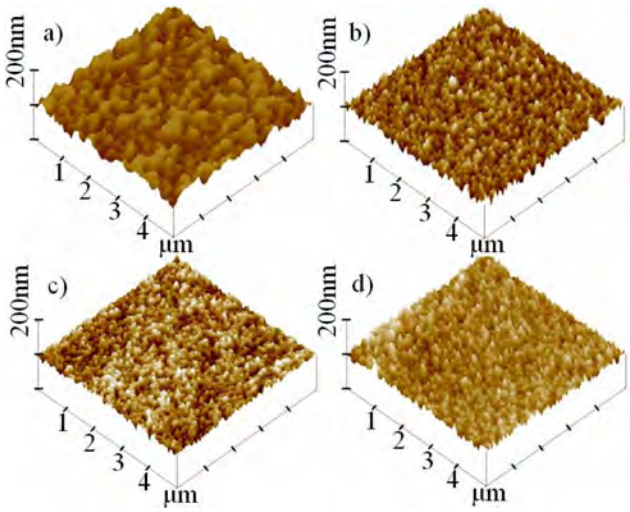

FIG. 6. (Color online) Influence of coil currents on the surface morphology: (a) 0 A, (b) 2 A, (c) 4 A, and (d) 6 A.

morphology and microstructure substantially. A homogeneous and noncolumnar structure is present throughout the film, and the surface roughness decreases. Similar results have been reported by Chakrabarti *et al.*[32] and Shew *et al.*[22] The proper nitrogen flow rate gives rise to a dense and fine morphology. If the coil current is increased (e.g., to 4 A), the film shows the compact morphology and low roughness. However, further increasing the coil current to 6 A roughens the surface due to formation of AlN and resputtering changes the film growth mechanism.

Figure 7 displays the nanohardness and modulus variations with coil currents. The surface hardness increases appreciably in the presence of the external magnetic field.

A maximum hardness of 28 GPa is achieved at a coil current of 4 A due to the denser structure, smaller crystal size, and more nitrogen incorporation as consistent with trend in plasma-enhanced magnetron sputtering (PEMS)[33] in which an ion flux 25 times that of conventional magnetron sputtering has been observed.[34] The enhanced hardness can be correlated to the microstructure and ion bombardment. Erkens *et al.*[24] have reported that by using plasma-enhanced

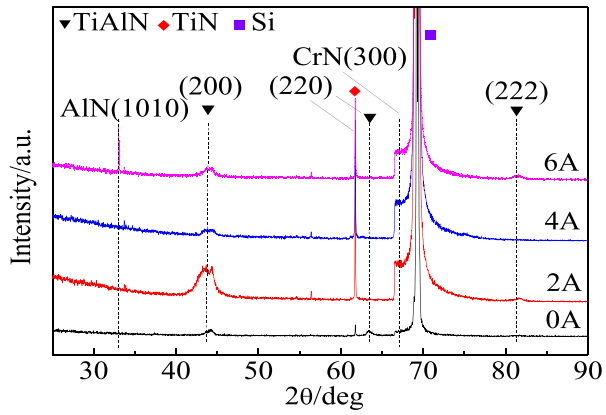

FIG. 5. (Color online) X-ray diffraction patterns acquired from the $(AlTi)_xN_{1-x}$ films deposited on silicon.

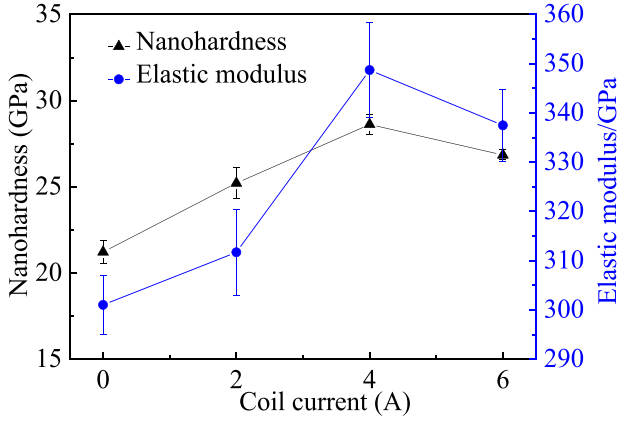

FIG. 7. (Color online) Effects of coil currents on the nanohardness and modulus.

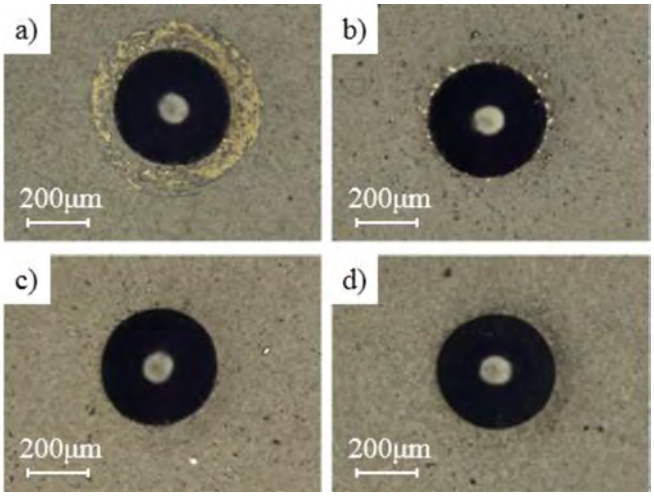

FIG. 8. (Color online) Effect of coil currents on adhesion strength between the film and substrate: (a) 0 A, (b) 2 A, (c) 4 A, and (d) 6 A.

sputtering, supernitride coatings with a dense and nanostructured morphology, appropriate surface finish, and good adhesion are produced. Similar to PEMS, HiPIMS assisted by an external magnetic field produces a larger ion flux to improve the mechanical and tribological properties of the coatings. However, an excessively high coil current leads to lower hardness on account of precipitation of AlN. Oliveira *et al.*[35] have shown that the AlN layer has a nanohardness between 12.5 and 16 GPa, which is lower than that of TiN or AlTiN. The lower hardness may be related to the influence of the magnetic field on the Ti charge state[36] which affects the bombardment dynamics and flux-controlled growth of TiAlN.[7] For instance, the doubly ionized metal flux is much larger from the Ti target than an Al one in HiPIMS.[37] This may be another reason for lower titanium concentration in the deposited films due to intensive back-attraction effect of ions with higher charge state.

The external magnetic field improves film adhesion. Figure 8 shows the Rockwell adhesion tests conducted on the $(AlTi)_xN_{1-x}$ coatings. According to the Daimler–Benz adhesion quality rankings and standards in the VDI guidelines 3198(1991), the coatings deposited using coil currents of 4 and 6 A are accepted by HF1, the highest adhesion value. However, if the coil current is lower or zero, adhesion is weak (HF6 for the sample without magnetic field and HF4 for the sample deposited at a coil current of 2 A). Figure 9 displays a similar trend from the scratch test with a maximum load of 50 N showing that a larger coil current produces better film adhesion. According to the scratch test, the critical load of the $(AlTi)_xN_{1-x}$ film prepared without the magnetic field is only 31 N but that produced using a coil current of 6 A is 50 N. Figure 10 displays the friction results from the ball-on-disk test. As the coil current goes up, the friction coefficient decreases and at a coil current of 6 A, the friction coefficient is as small as 0.28. The enhancement may be related to the formation of AlN as reported previously.[38,39]

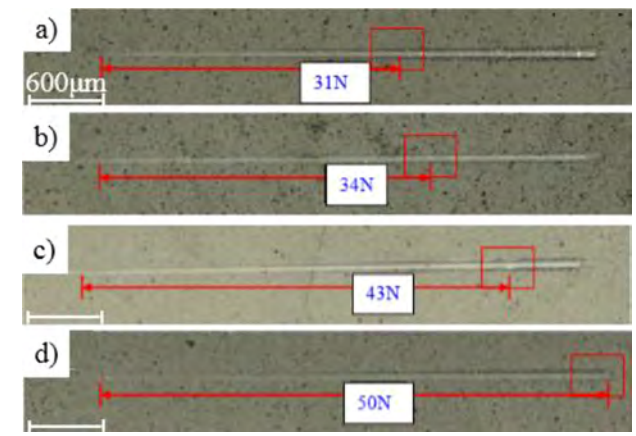

FIG. 9. (Color online) Critical loads of the $(AlTi)_xN_{1-x}$ films for different coil currents: (a) 0 A, (b) 2 A, (c) 4 A, and (d) 6 A. All scar bars are 600 μm.

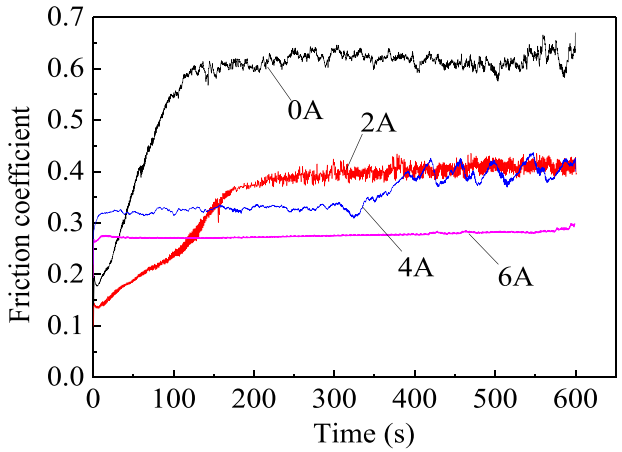

FIG. 10. (Color online) Friction coefficients of the $(AlTi)_xN_{1-x}$ films deposited using different coil currents.

IV. CONCLUSION

HiPIMS is performed in the presence of an external magnetic field which enhances the plasma density near the substrate and bias current. This magnetic field also increases nitrogen incorporation into the $(AlTi)_xN_{1-x}$ film producing a smoother surface (5.2 nm), higher hardness (28 GPa), and better film adhesion (HF1 and at least Lc > 50 N). A higher deposition rate is also observed in the presence of the magnetic field which can be used controllably to improve the efficiency of HiPIMS as well as structure and properties of the deposited films.

ACKNOWLEDGMENTS

This work was financially supported by Natural Science foundation of China ((Nos. U1330110, 11675047 and 51175118), Hong Kong Research Grants Council (RGC) General Research Funds (GRF) No. CityU 11301215, as well as City University of Hong Kong Applied Research Grant (ARG) No. 9667104.

[1]P. J. Kelly and R. D. Arnell, Vacuum **56**, 159 (2000).
[2]V. Kouznetsov, K. Macak, J. M. Schneider, U. Helmersson, and I. Petrov, Surf. Coat. Technol. **122**, 290 (1999).
[3]U. Helmersson, M. Lattemann, J. Bohlmark, A. P. Ehiasarian, and J. T. Gudmundsson, Thin Solid Films **513**, 1 (2006).

[4]K. Sarakinos, J. Alami, and S. Konstantinidis, Surf. Coat. Technol. **204**, 1661 (2010).
[5]R. Bandorf, V. Sittinger, and G. Bräuer, "High power impulse magnetron sputtering-HIPIMS," in *Comprehensive Materials Processing* (Elsevier, Oxford, 2014), Vol. 4, pp. 75–99.
[6]F. Papa, H. Gerdes, R. Bandorf, A. P. Ehiasarian, I. Kolev, G. Braeuer, R. Tietema, and T. Krug, Thin Solid Films **520**, 1559 (2011).
[7]G. Greczynski, J. Lu, J. Jensen, S. Bolz, W. Koelker, C. Schiffers, O. Lemmer, J. E. Greene, and L. Hultman, Surf. Coat. Technol. **257**, 15 (2014).
[8]B. Martin and F. Martin, Surf. Coat. Technol. **250**, 37 (2014).
[9]J. Emmerlich, S. Mraz, R. Snyders, K. Jiang, and J. M. Schneider, Vacuum **82**, 867 (2008).
[10]L. Velicu, V. Tiron, and G. Popa, Surf. Coat. Technol. **250**, 57 (2014).
[11]J. Capek, M. Hala, O. Zabeida, J. E. Klemberg-Sapieha, and L. Martinu, J. Phys. D: Appl. Phys. **46**, 205205 (2013).
[12]A. Anders, Surf. Coat. Technol. **257**, 308 (2014).
[13]G. Kamath, A. P. Ehiasarian, Y. Purandare, and P. E. Hovsepian, Surf. Coat. Technol. **205**, 2823 (2011).
[14]J. L. Endrino, G. S. Fox-Rabinovich, and C. Gey, Surf. Coat. Technol. **200**, 6840 (2006).
[15]P. Budzynski, J. Sielanko, and Z. Surowie, Intermetallics **16**, 987 (2008).
[16]Z. Z. Wu, X. B. Tian, J. W. Shi, Z. M. Wang, C. Z. Gong, S. Q. Yang, and P. K. Chu, Rev. Sci. Instrum. **82**, 033511 (2011).
[17]T. Weirather, K. Chladil, B. Sartory, D. Caliskanoglu, R. Cremer, W. Kölker, and C. Mitterer, Surf. Coat. Technol. **257**, 48 (2014).
[18]A. Anders and I. Brown, IEEE Trans. Plasma Sci. **39**, 2528 (2011).
[19]T. Jager, Y. E. Romanyuk, A. N. Tiwari, and A. Anders, J. Appl. Phys. **116**, 033301 (2014).
[20]A. Anders, Surf. Coat. Technol. **205**, S1 (2011).
[21]L. Chen, M. Moser, Y. Du, and P. H. Mayrhofer, Thin Solid Films **517**, 6635 (2009).
[22]B. Y. Shew and J. L. Huang, Surf. Coat. Technol. **71**, 30 (1995).
[23]K. Tönshoff, B. Karpuschewski, A. Mohlfeld, T. Leyendecker, G. Erkens, H. G. Fuß, and R. Wenke, Surf. Coat. Technol. **108**, 535 (1998).
[24]G. Erkens, Surf. Coat. Technol. **201**, 4806 (2007).
[25]K. D. Bouzakis, G. Skordaris, N. Michailidis, I. Mirisidis, G. Erkens, and R. Cremer, Surf. Coat. Technol. **202**, 826 (2007).
[26]E. Lewin, D. Loch, A. Montagne, A. P. Ehiasarian, and J. Patscheider, Surf. Coat. Technol. **232**, 680 (2013).
[27]J. Bohlmark, M. Östbye, M. Lattemann, H. Ljungcrantz, T. Rosell, and U. Helmersson, Thin Solid Films **515**, 1928 (2006).
[28]P. J. Kelly and R. D. Arnell, Surf. Coat. Technol. **108**, 317 (1998).
[29]C. Strondl, G. J. Kolk, T. Hurkmanns, W. Fleischer, T. Trinh, N. M. Carvalho, and J. T. Hosson, Surf. Coat. Technol. **142**, 707 (2001).
[30]V. Uvarov and I. Popov, Mater. Charact. **58**, 883 (2007).
[31]F. Ferreira, R. Serra, J. C. Oliveira, and A. Cavaleiro, Surf. Coat. Technol. **258**, 249 (2014).
[32]K. Chakrabarti, J. J. Jeong, S. K. Hwang, Y. C. Yoo, and C. M. Lee, Thin Solid Films **406**, 159 (2002).
[33]A. M. A. El-Rahman and R. H. Wei, Surf. Coat. Technol. **241**, 74 (2014).
[34]R. H. Wei, E. Langa, C. Rincon, and J. H. Arps, Surf. Coat. Technol. **201**, 4453 (2006).
[35]I. C. Oliveira, K. G. Grigorov, H. S. Maciel, M. Mass, and C. Otani, Vacuum **75**, 331 (2004).
[36]I. A. Krinberg and G. K. Matafonov, Surf. Coat. Technol. **201**, 8615 (2007).
[37]G. Greczynski, J. Lu, M. P. Johansson, J. Jensen, I. Petrov, J. E. Greene, and L. Hultman, Surf. Coat. Technol. **206**, 4202 (2012).
[38]Z. G. Wu, G. A. Zhang, M. X. Wang, X. Y. Fan, P. X. Yan, and T. Xu, Appl. Surf. Sci. **253**, 2733 (2006).
[39]P. F. Yang, S. R. Jian, S. Wu, Y. S. Lai, C. T. Wang, and R. S. Chen, Appl. Surf. Sci. **255**, 5984 (2009).